

Combination of mesoporous titanium dioxide with MoS₂ nanosheets for high photocatalytic activity

Loghman Karimi

Young Researchers and Elites Club, Science and Research Branch, Islamic Azad University, Tehran, Iran
Corresponding author: e-mail: l.karimi@srbiau.ac.ir

This study presents a facile approach for the preparation of MoS₂ nanosheet decorated by porous titanium dioxide with effective photocatalytic activity. Mesoporous titanium dioxide nanostructures first synthesized by a hydrothermal process using titanium (III) chloride and then the MoS₂/TiO₂ were prepared through mixing of MoS₂ nanosheet with mesoporous titanium dioxide under ultrasonic irradiation. The synthesized nanocomposite was characterized by X-ray diffraction (XRD), transmission electron microscopy (TEM), field emission scanning electron microscopy (FE-SEM), and Brunauer-Emmett-Teller (BET) analysis. The results showed that the nanocomposite has mesoporous structure with specific surface area of 176.4 m²/g and pore diameter of 20 nm. The as-prepared MoS₂/TiO₂ nanocomposites exhibited outstanding photocatalytic activity for dye degradation under sunlight irradiation, which could be attributed to synergistic effect between the molybdenum disulfide nanosheet and mesoporous titanium dioxide. The photocatalytic performance achieved is about 2.2 times higher than that of mesoporous TiO₂ alone. It is believed that the extended light absorption ability and the large specific surface area of the 2D MoS₂ nanosheets in the nanocomposite, leading to the enhanced photocatalytic degradation activity.

Keywords: MoS₂ nanosheet, mesoporous titanium dioxide, photocatalytic, ultrasound, direct green 6.

INTRODUCTION

Photocatalytic decomposition of toxic and hazardous organic pollutants using semiconductor photocatalysts has attracted considerable interest, because it offers enormous potential for the protection of environment^{1,2}. Among the semiconductor materials, nano titanium dioxide (TiO₂) is widely used for its relatively high photocatalytic activity, low cost, physical and chemical stability, nontoxicity and potential applications in photo/photoelectrocatalytic degradation of pollutants, hydrogen production, supercapacitors, dye-sensitized solar cells, sensors, and biomedical devices³⁻⁷. When the photocatalyst is illuminated by a light source with energy higher than its bandgap energy, electron-hole pairs diffuse out to the surface of the photocatalyst. The generated negative electrons and oxygen combine into O₂⁻, and the positive electric holes and water generate hydroxyl radicals. These highly active oxygen species can oxidize organic pollutants. Thus, titanium dioxide can photocatalytically decompose dye molecules and common organic matters such as odor molecules, bacteria and viruses⁸.

Although there are numerous advantages in utilizing the titanium dioxide, there are some disadvantages for the pure one as follows: The photogenerated electron-hole pairs have a flash recombination time on the order of 10⁻⁹ s, while the time scale of chemical interactions of TiO₂ with the adsorbed dye or chemicals are in the slower range of 10⁻⁸ to 10⁻³ s. This discrepancy between two time scales results in an unintended recombination of electron-hole pairs, leading to decreased efficiency in the photocatalytic activity of TiO₂⁹. Also, titanium dioxide only shows photocatalytic activities under ultraviolet irradiation¹⁰. Extensive research regarding the modification of photocatalytic performance of titanium dioxide has been conducted. Some studies have focused on the combination of titanium dioxide and carbonaceous materials for producing nanocomposites, i.e. graphene/TiO₂^{11, 12}, carbon black/TiO₂¹³, and carbon nanotube/TiO₂^{14, 15}. Also, some noble metals such as Pt^{16, 17}, Au^{18, 19},

and Ag^{20, 21} have been used for modifying the photocatalytic properties of titanium dioxide. The enhancement in photocatalytic performance of titanium dioxide occurs through mitigating the rate of electrons and holes recombination by trapping the electrons, expanding the light efficiency into visible territory, and modifying the surface properties of photocatalysts by deposition of cocatalysts to reduce activation energy^{22, 23}.

There have been some reports on the usage of molybdenum disulfide/titanium dioxide nanocomposite in photocatalysis process. For instance, Bai et al. prepared TiO₂-MoS₂ hybrid structure with excellent performance in both photocatalytic hydrogen production and Rhodamine B degradation²⁴. Along the same lines, Zhang et al. obtained TiO₂/MoS₂ composite photocatalyst via a one-step hydrothermal process using titanium tetrachloride (TiCl₄) as a titanium dioxide precursor and bulk MoS₂ as a direct photosensitizer²⁵. Thin films with hetero-structure of MoS₂/TiO₂ are studied at the interface to determine the electronic behavior by Tao and coworkers²⁶. Ren et al. presented facile hydrothermal process for preparation of 2D photocatalytic TiO₂/MoS₂ hybrid nanosheets²⁷. Zhou et al. coated TiO₂ nanobelt heterostructures with MoS₂ nanosheet for enhance photocatalytic activities²⁸. Shen and coworkers fabricated MoS₂ nanosheet/TiO₂ nanowire hybrid nanostructures and obtained photocatalyst with high activity under visible light irradiation²⁹. Loading of 2D MoS₂ nanosheets on the surface of 2D anatase TiO₂ nanosheets was reported by Yuan et al.³⁰. Liu et al. synthesized MoS₂/TiO₂ nanocomposite with superior photocatalytic activity in hydrogen production³¹. Also, the photodegradation of methyl orange in aqueous solution with nano-MoS₂/TiO₂ composite was investigated by Hu and colleagues³². However, the photocatalytic performance of MoS₂ nanosheets/mesoporous titanium dioxide composite has not been reported yet.

In this study, mesoporous TiO₂ was synthesized through the hydrothermal approach by applying titanium (III) chloride as titanium dioxide precursor and then the MoS₂

nanosheets/mesoporous titanium dioxide composite was prepared by a simple method of mixing and sonication. The photocatalytic activity of the synthesized photocatalysts was examined by monitoring the degradation of an azo textile dye (direct green 6).

EXPERIMENTAL

Chemicals

Molybdenum (IV) sulfide powder with particle size of less than 2 μm and poly(vinylpyrrolidone) (PVP, average mol wt 40.000) were purchased from Sigma-Aldrich Co. Titanium (III) chloride solution (TiCl_3 , 15% in about 10% hydrochloric acid) and 1-methyl-2-pyrrolidone ($\text{C}_5\text{H}_9\text{NO}$, 99.5%) were prepared by Merck Co. Commercially available direct green 6 (CI 30295) was obtained from Alvan Sabet Co. (Iran). Deionized water was used throughout this study.

Methods

(1) Synthesis of MoS_2 nanosheets:

The MoS_2 nanosheets dispersions were prepared based on the Coleman's method via a liquid phase exfoliation technique^{33, 34}. Molybdenum (IV) sulfide powder was added to 1-methyl-2-pyrrolidone solvent at a concentration ratio of 10 mg/mL. The mixture was then sonicated continuously for 60 minutes at 25% amplitude with a horn probe sonic tip (VibraCell CVX, 750W, 25% amplitude) while ice-cooling the dispersion. The final sonicated dispersion was centrifuged at 3000 rpm for 30 min to remove non-exfoliated MoS_2 sheets, the supernatant was then decanted.

(2) Synthesis of mesoporous titanium dioxide:

To synthesize of mesoporous titanium dioxide, 5 mL of titanium trichloride aqueous solution as precursor and 300 mg of poly(vinylpyrrolidone) were added to 100 mL water while stirring. The mixture was stirred at 95°C for 60 min. The suspension was then reacted hydrothermally in a 100 mL Teflon-lined autoclave at 200°C for 6 h. After that, the precipitate was harvested by centrifugation, followed by washing with ethanol and water three times.

(3) Synthesis of $\text{MoS}_2/\text{TiO}_2$ nanocomposite:

Different amounts of the mesoporous titanium dioxide (0.05, 0.1, 0.2, 0.3, 0.4, 0.5 wt.%) were added to the MoS_2 suspension (100 mL) and sonicated in an ultrasonic bath (Euronada Eurosonic® 4D) under 50/60 Hz frequency for 60 min. After the completion of mixing, the resulting products were filtered and washed with distilled water, and then dried at 50°C for 24 h.

Characterization

Morphologies of the samples were observed by using a field emission scanning electron microscope (FESEM, MIRA3-TESCAN, Czech Republic). X-ray diffraction (XRD, STOE, model STADI MP, Germany) was used to survey the crystal compositions and crystal sizes. Transmission electron microscopy (TEM) images of the samples were obtained on a Phillips EM208 electron microscope, Czech Republic. The surface area and pore size distribution were investigated with a Gemini III 2375 apparatus. The standard multi-points Brunauer–

Emmett–Teller (BET) method was utilized to calculate the specific surface area. The pore size distributions of the materials were derived from the adsorption branches of the isotherms based on the Barrett–Joyner–Halenda (BJH) model.

Photocatalytic degradation of direct green⁶

In order to investigate the photocatalytic performance of the samples, decrease in concentration drop of the direct green⁶ during exposure to sunlight was analyzed. The concentration of dye in the solution was calculated by a Varian Cary 300 UV-Vis spectrophotometer using a calibration curve (containing seven points). A computer program determines the absorbance of the dye solution at the maximum wavelength of direct green 6–623 nm. The first step was the preparation of dye solution by distilled water (60 mg/L). Then, the nano materials were added to 100 mL of the dye solution. First, the solution mixture was stirred for 15 min without irradiation in order to obtain equilibrium of dye adsorption. Then, the solution was irradiated under sunlight (with approximate light intensity of 0.75 W m^{-2}) for 3 consecutive days. The dye solution was continuously stirred at a rate of 200 rpm and the real dye solution was maintained at pH (6.6). After irradiation, the samples were purified with Millipore filter. The decolorization and photocatalytic degradation efficiencies were calculated as:

$$\text{Efficiency (\%)} = (C_0 - C_e) / C_e \times 100 \quad (1)$$

where C_0 and C_e correspond to the initial and final concentration of dye before and after sunlight irradiation. In this equation $E\%$ shows the dye photocatalyst degradation percent³⁵.

RESULTS AND DISCUSSION

Figure 1A shows the FE-SEM image of the prepared titanium dioxide, indicating that a large amount of TiO_2

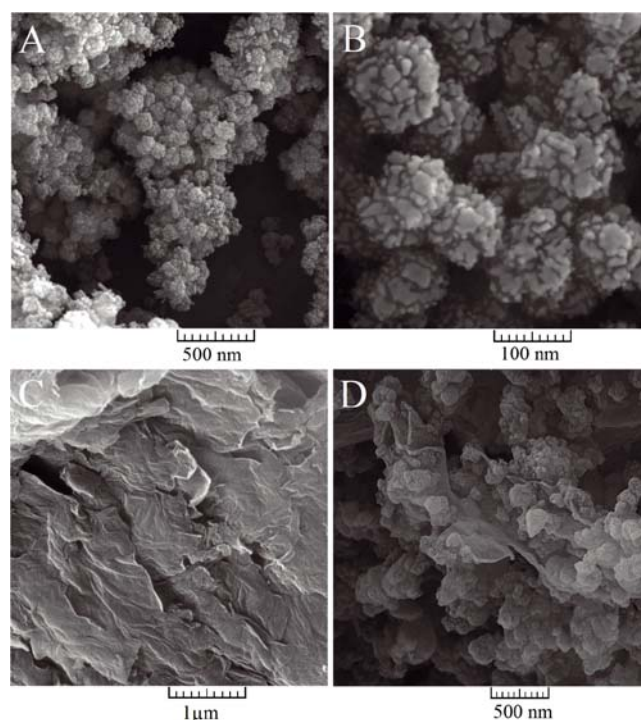


Figure 1. FE-SEM images of the prepared samples: (A, B) mesoporous titanium dioxide, (C) MoS_2 sheets and (D) $\text{MoS}_2/\text{TiO}_2$ nanocomposite

nanoparticles are generated with homogeneous and spherical morphology. The high-magnification of the individual spheres (Fig. 1B) reveals that the mesoporous titania is formed by aggregated clusters consisting of nanoparticles, and this is how the disorder mesoporous structure is formed. The mesoporous titanium dioxide nanoparticles are recognized on the surface of MoS₂ flakes via comparing Figure 1C with Figure 1D.

As seen in Figure 2A, the pore structure is observed at the space between TiO₂ nanoparticles, indicating the inter-particle porosity is due to the mesoporosity. This result is consistent with the FE-SEM images. Also, through the TEM images of MoS₂ nanosheets and MoS₂/TiO₂ nanocomposite (Fig. 2B, C), the presence of mesoporous TiO₂ on the molybdenum disulfide nanosheets was confirmed. Moreover, Figure 2C shows that the MoS₂ sheets are densely decorated with titania.

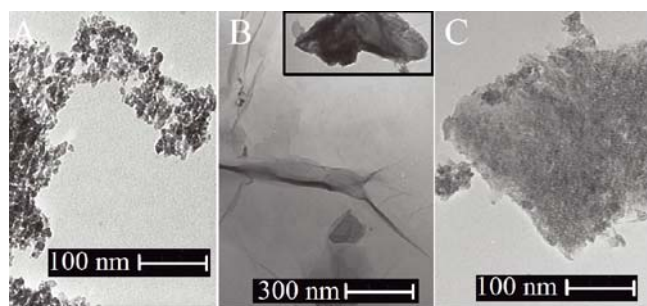


Figure 2. TEM images of (A) mesoporous titanium dioxide, (B) MoS₂ nanosheets and (C) MoS₂/TiO₂ nanocomposite

X-ray diffraction was used to determine the crystal status and crystal size of the prepared nanocomposite. XRD pattern (Fig. 3) indicates that the MoS₂ nanosheets/mesoporous titanium dioxide composite with well-defined crystallinity consist of hexagonal phase MoS₂ and anatase phase TiO₂. In addition, based on equation (2), the crystal size was calculated at $2\theta = 25.3^\circ$ and for the nanocomposite was 178 Å.

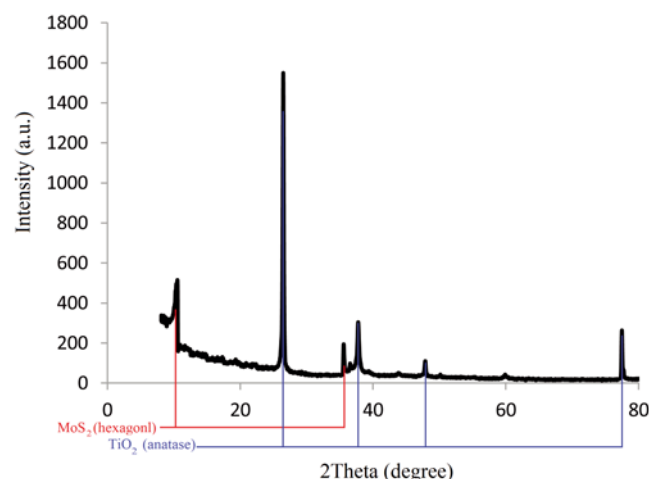


Figure 3. XRD pattern of MoS₂/TiO₂ nanocomposite

Crystal size (Å) = $(K \times \lambda \times 180) / (\text{FWHM} \times \pi \times \cos \theta)$ (2) where $K = 0.9$ is the shape factor, $\lambda = 1.54$ is the wavelength of X-ray of Cu radiation, FWHM is full width at half maximum of the peak, and θ is the diffraction angle³⁶.

The specific surface areas and pore size distributions of the nanocomposite have been characterized using nitrogen adsorption and desorption isotherm as shown

in Figure 4. The isotherm of the sample is in good agreement with type (IV) isotherms, indicating the presence of mesoporous material according to the IUPAC classification^{37, 38}. Furthermore, the nanocomposite had a specific surface area of 176.4 m²/g and a narrow pore size distribution centered at 20 nm.

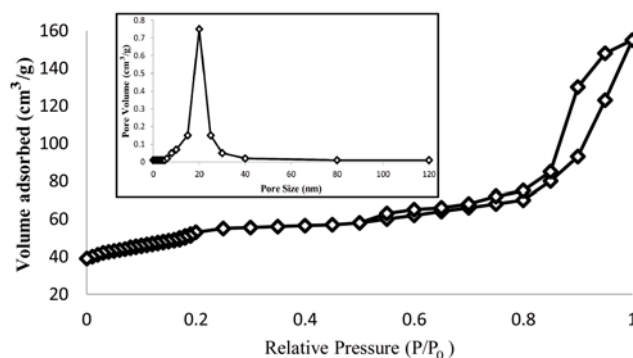


Figure 4. Nitrogen sorption isotherm of the MoS₂/TiO₂ nanocomposite. Inset shows the corresponding pore diameter distribution

The photocatalytic activity of mesoporous titanium dioxide and MoS₂/TiO₂ nanocomposite was examined by the degradation of direct green 6 (Fig. 5) solutions under sunlight irradiation. More than 50% of textile dyes is azo dyes. About 20% of dye products enter into textile wastewater during the dyeing process³⁹. Direct green 6 is an aromatic azo compound with molecular formula C₃₄H₂₂N₈Na₂O₉S₂. It has many uses in textiles dyeing, such as clothes or leathers. This dye is stable, incompatible with bases, reducing agents and strong oxidizing agents. Since azo bonds are the chromophores contributing to color of azo dyes, decolorization of the azo dyes is very likely influenced by the number of azo bonds present in a dye molecule. Generally speaking, trisazo dyes like direct green 6 are refractory.

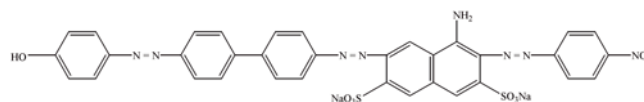


Figure 5. Structure formula of direct green 6 azo dye

Figure 6 illustrates photo-degradation of direct green 6 with mesoporous titanium dioxide or MoS₂/TiO₂ nanocomposite in the different dosage of titanium dioxide. As shown in Figure 6A, the discoloration rate of the direct green 6 solution increased with increasing contents of the mesoporous titanium dioxide. Generally, the catalytic capability can be improved with increasing amounts of the catalyst. The azo dye used in this study was anionic dye and was negatively charged because of the sulfonate groups (Fig. 5). Accordingly, electrostatic interactions between the photocatalysts surface (Ti³⁺) and dye anions lead to the adsorption of dye molecule on the surface^{8, 40}. Compared with bulk TiO₂, the mesoporous TiO₂ enhances the density of accessible active sites for dye adsorption and decomposition⁴¹. Thus, the adsorbed dye molecules on the surface of the catalyst degraded completely due to generations of highly oxidative species by titanium dioxide under irradiation.

Based on the obtained results (Fig. 6B), adding molybdenum disulfide nanosheets to mesoporous titanium

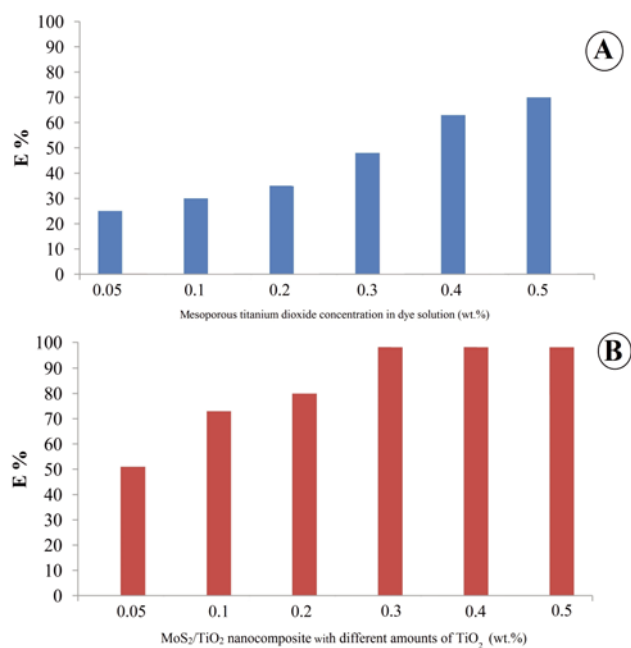


Figure 6. The photocatalytic efficiency of mesoporous titanium dioxide (A) and MoS₂/TiO₂ nanocomposites (B)

dioxide had a tangible effect on the photocatalytic performance of photocatalyst and its photocatalytic degradation efficiency was higher than that of mesoporous TiO₂ under sunlight irradiation. It could be a result of the large surface area of 2D MoS₂ nanosheets. The 2D nanomaterials as compared to 1D or 0D nanostructures may provide a better anchoring surface for adsorbing molecules²⁸. Furthermore, the extended light absorption ability of MoS₂/TiO₂ nanocomposite improves the photocatalytic performance³². The possible reactions for MoS₂/TiO₂ nanocomposite under sunlight irradiation can be summarized as follows.

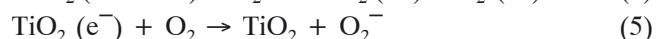
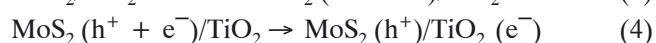
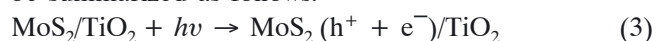


Figure 6B showed that by increasing the amount of mesoporous TiO₂, degradation of dye was increased but practically there was no degradation more than 0.3 wt.% mesoporous titanium dioxide, which is due to the aggregation of synthesized titanium dioxide on MoS₂ nanosheets. Therefore, besides being more cost effective compared with 0.5% TiO₂, 0.3% TiO₂ provided an optimal effect on the photocatalytic performance of the prepared nanocomposite.

CONCLUSIONS

In summary, highly crystallized molybdenum disulfide/mesoporous titanium dioxide nanocomposite with large surface areas of 176.4 m²/g and narrow pore size distribution of 20 nm have been prepared through a combined hydrothermal and sonosynthesis process. Through FE-SEM and TEM images, BJH and BET analyses,

and XRD pattern the successful synthesis of MoS₂/TiO₂ nanocomposite was verified. Such nanocomposite possesses strong adsorption ability and high photocatalytic performance in the degradation of direct green 6 as an azo dye. On the composite system, the positive synergetic effect between the MoS₂ nanosheets and mesoporous TiO₂ can efficiently extend light absorption ability and provide a greater number of active adsorption sites. It is expected MoS₂/TiO₂ nanocomposite can be used as the superior photocatalyst, especially for environmental and clean energy applications.

LITERATURE CITED

- Hoffmann, M.R., Martin, S.T., Choi, W. & Bahnemann, D.W. (1995). Environmental applications of semiconductor photocatalysis. *Chem. Rev.* 95(1), 69–96. DOI: 10.1021/cr00033a004.
- Serpone, N. & Emeline, A.V. (2012). Semiconductor photocatalysis—past, present, and future outlook. *J. Phys. Chem. Lett.* 3(5), 673–677. DOI: 10.1021/jz300071j.
- Gholami, T., Salavati-Niasari, M., Reza Momenian, H., Noori, E. & Ghanbari, D. (2015). Synthesis of Titanium Dioxide Nanoparticles and Investigation of Its Photocatalytic Properties. *Synth. React. Inorg. M.* 45(7), 1092–1096. DOI: 10.1080/15533174.2013.862670.
- Chen, X. & Selloni, A. (2014). Introduction: titanium dioxide (TiO₂) nanomaterials. *Chem. Rev.*, 114(19), 9281–9282. DOI: 10.1021/cr500422r.
- Ge, M.Z., Cao, C.Y., Huang, J.Y., Li, S.H., Zhang, S.N., Deng, S., Li, Q.S., Zhang, K.Q. & Lai, Y.K. (2016). Synthesis, modification, and photo/photoelectrocatalytic degradation applications of TiO₂ nanotube arrays: a review. *Nanotechnol. Rev.* 5(1), 75–112. DOI: 10.1515/ntrev-2015-0049.
- Jafari, T., Moharreri, E., Amin, A.S., Miao, R., Song, W. & Suib, S.L. (2016). Photocatalytic water splitting—the untamed dream: a review of recent advances. *Molecules* 21(7), 900. DOI: 10.3390/molecules21070900.
- Wen, J., Li, X., Liu, W., Fang, Y., Xie, J. & Xu, Y. (2015). Photocatalysis fundamentals and surface modification of TiO₂ nanomaterials. *Chinese J. Catal.* 36(12), 2049–2070. DOI: 10.1016/S1872-2067(15)60999-8.
- Zohoori, S., Karimi, L. & Ayazi Yazdi, S. (2014). A novel durable photoactive nylon fabric using electrospun nanofibers containing nanophotocatalysts. *J. Indus. Eng. Chem.* 20(5), 2934–2938. DOI: 10.1016/j.jiec.2013.10.062.
- Sher Shah, M.S.A., Park, A.R., Zhang, K., Park, J.H. & Yoo, P.J. (2012). Green synthesis of biphasic TiO₂-reduced graphene oxide nanocomposites with highly enhanced photocatalytic activity. *ACS Appl. Mater. Interfaces* 4(8), 3893–3901. DOI: 10.1021/am301287m.
- Pelaez, M., Nolan, N.T., Pillai, S.C., Seery, M.K., Falaras, P., Kontos, A.G., Dunlop, P.S., Hamilton, J.W., Byrne, J.A., O'shea, K. & Entezari, M.H. (2012). A review on the visible light active titanium dioxide photocatalysts for environmental applications. *Appl. Catal. B.* 125, 331–349. DOI: 10.1016/j.apcatb.2012.05.036.
- Perera, S.D., Mariano, R.G., Vu, K., Nour, N., Seitz, O., Chabal, Y. & Balkus Jr, K.J. (2012). Hydrothermal synthesis of graphene-TiO₂ nanotube composites with enhanced photocatalytic activity. *ACS Catal.* 2(6), 949–956. DOI: 10.1021/cs200621c.
- Posa, V.R., Annaram, V., Koduru, J.R., Bobbala, P. & Somala, A.R. (2016). Preparation of graphene-TiO₂ nanocomposite and photocatalytic degradation of Rhodamine-B under solar light irradiation. *J. Exp. Nanosci.* 11(9), 722–736. DOI: 10.1080/17458080.2016.1144937.
- Li, L., Zhu, W., Zhang, P., Chen, Z. & Han, W. (2003). Photocatalytic oxidation and ozonation of catechol over carbon-black-modified nano-TiO₂ thin films supported on Al

- sheet. *Water Res.* 37(15), 3646–3651. DOI: 10.1016/S0043-1354(03)00269-0.
14. Nguyen, V.H., Ren, Y., Lee, Y.R., Tuma, D., Min, B.K. & Shim, J.J. (2012). Microwave-assisted synthesis of carbon nanotube-TiO₂ nanocomposites in ionic liquid for the photocatalytic degradation of methylene blue. *Synth. React. Inorg. M.* 42(2), 296–301. DOI: 10.1080/15533174.2011.610021.
15. Rath, P.C., Nayak, S., Bhattacharjee, S., Besra, L. & Singh, B.P. (2014). Nanotitania-coated multi-walled carbon nanotube composite by facile colloidal processing route for photocatalytic applications. *Compos. Interfaces* 21(3), 251–262. DOI: 10.1080/15685543.2014.864530.
16. Chowdhury, P., Malekshoar, G., Ray, M.B., Zhu, J. & Ray, A.K. (2013). Sacrificial hydrogen generation from formaldehyde with Pt/TiO₂ photocatalyst in solar radiation. *Indus. Eng. Chem. Res.* 52(14), 5023–5029. DOI: 10.1021/ie3029976.
17. Zhang, F., Xie, F., Fang, T., Zhang, K., Chen, T. & Oh, W. (2012). Photocatalytic Degradation of Methyl Orange on Platinum and Palladium Co-doped TiO₂ Nanoparticles. *Synth. React. Inorg. M.* 42(5), 685–691. DOI: 10.1080/15533174.2011.615040.
18. Li, X., Huang, T., Luo, K., Zhang, P., Li, Z. & Liang, C. (2013). Synthesis and catalytic property of Au/titania nanocomposites on the photocatalytic degradation of methyl orange. *Synth. React. Inorg. M.* 43, 367–372. DOI: 10.1080/15533174.2012.740726.
19. Miljevic, M., Geiseler, B., Bergfeldt, T., Bockstaller, P. & Fruk, L. (2014). Enhanced photocatalytic activity of Au/TiO₂ nanocomposite prepared using bifunctional bridging linker. *Adv. Funct. Mater.* 24(7), 907–915. DOI: 10.1002/adfm.201301484.
20. Lu, Q., Lu, Z., Lu, Y., Lv, L., Ning, Y., Yu, H., Hou, Y. & Yin, Y. (2013). Photocatalytic synthesis and photovoltaic application of Ag-TiO₂ nanorod composites. *Nano Lett.* 13(11), 5698–5702. DOI: 10.1021/nl403430x.
21. Yang, D., Sun, Y., Tong, Z., Tian, Y., Li, Y. & Jiang, Z. (2015). Synthesis of Ag/TiO₂ nanotube heterojunction with improved visible-light photocatalytic performance inspired by bioadhesion. *J. Phys. Chem. C* 119(11), 5827–5835. DOI: 10.1021/jp511948p.
22. Leary, R. & Westwood, A. (2011). Carbonaceous nanomaterials for the enhancement of TiO₂ photocatalysis. *Carbon* 49(3), 741–772. DOI: 10.1016/j.carbon.2010.10.010.
23. Kumar, S.G. & Devi, L.G. (2011). Review on modified TiO₂ photocatalysis under UV/visible light: selected results and related mechanisms on interfacial charge carrier transfer dynamics. *J. Phys. Chem. A* 115(46), 13211–13241. DOI: 10.1021/jp204364a.
24. Bai, S., Wang, L., Chen, X., Du, J. & Xiong, Y. (2015). Chemically exfoliated metallic MoS₂ nanosheets: A promising supporting co-catalyst for enhancing the photocatalytic performance of TiO₂ nanocrystals. *Nano Res.* 8(1), 175–183. DOI: 10.1007/s12274-014-0606-9.
25. Zhang, W., Xiao, X., Zheng, L. & Wan, C. (2015). Fabrication of TiO₂/MoS₂ composite photocatalyst and its photocatalytic mechanism for degradation of methyl orange under visible light. *Can. J. Chem. Eng.* 93(9), 1594–1602. DOI: 10.1002/cjce.22245.
26. Tao, J., Chai, J., Guan, L., Pan, J. & Wang, S. (2015). Effect of interfacial coupling on photocatalytic performance of large scale MoS₂/TiO₂ hetero-thin films. *Appl. Phys. Lett.* 106(8), 081602. DOI: 10.1063/1.4913662.
27. Ren, X., Qi, X., Shen, Y., Xiao, S., Xu, G., Zhang, Z., Huang, Z. & Zhong, J. (2016). 2D co-catalytic MoS₂ nanosheets embedded with 1D TiO₂ nanoparticles for enhancing photocatalytic activity. *J. Phys. D: Appl. Phys.* 49(31), 315304. DOI: 10.1088/0022-3727/49/31/315304.
28. Zhou, W., Yin, Z., Du, Y., Huang, X., Zeng, Z., Fan, Z., Liu, H., Wang, J. & Zhang, H. (2013). Synthesis of few-layer MoS₂ nanosheet-coated TiO₂ nanobelt heterostructures for enhanced photocatalytic activities. *Small* 9(1), 140–147. DOI: 10.1002/smll.201201161.
29. Shen, M., Yan, Z., Yang, L., Du, P., Zhang, J. & Xiang, B. (2014). MoS₂ nanosheet/TiO₂ nanowire hybrid nanostructures for enhanced visible-light photocatalytic activities. *Chem. Commun.* 50(97), 15447–15449. DOI: 10.1039/C4CC07351G.
30. Yuan, Y.J., Ye, Z.J., Lu, H.W., Hu, B., Li, Y.H., Chen, D.Q., Zhong, J.S., Yu, Z.T. & Zou, Z.G. (2015). Constructing anatase TiO₂ nanosheets with exposed (001) facets/layered MoS₂ two-dimensional nanojunctions for enhanced solar hydrogen generation. *ACS Catal.* 6(2), 532–541. DOI: 10.1021/acscatal.5b02036.
31. Liu, Q., Pu, Z., Asiri, A. M., Qusti, A. H., Al-Youbi, A. O. & Sun, X. (2013). One-step solvothermal synthesis of MoS₂/TiO₂ nanocomposites with enhanced photocatalytic H₂ production. *J. Nanopart. Res.* 15(11), 1–7. DOI: 10.1007/s11051-013-2057-8
32. Hu, K.H., Hu, X.G., Xu, Y.F. & Sun, J.D. (2010). Synthesis of nano-MoS₂/TiO₂ composite and its catalytic degradation effect on methyl orange. *J. Mater. Sci.* 45(10), 2640–2648. DOI: 10.1007/s10853-010-4242-9.
33. O'Neill, A., Khan, U. & Coleman, J.N. (2012). Preparation of high concentration dispersions of exfoliated MoS₂ with increased flake size. *Chem. Mater.* 24(12), 2414–2421. DOI: 10.1021/cm301515z.
34. Coleman, J.N., Lotya, M., O'Neill, A., Bergin, S.D., King, P.J., Khan, U., Young, K., Gaucher, A., De, S., Smith, R.J. & Shvets, I.V. (2011). Two-dimensional nanosheets produced by liquid exfoliation of layered materials. *Science* 331, 568–571. DOI: 10.1126/science.1194975.
35. Karimi, L., Zohoori, S. & Yazdanshenas, M.E. (2014). Photocatalytic degradation of azo dyes in aqueous solutions under UV irradiation using nano-strontium titanate as the nanophotocatalyst. *J. Saudi Chem. Soc.* 18(5), 581–588. DOI: 10.1016/j.jscs.2011.11.010.
36. Shirgholami, M.A., Karimi, L. & Mirjalili, M. (2016). Multifunctional modification of wool fabric using graphene/TiO₂ nanocomposite. *Fiber. Polym.* 17(2), 220–228. DOI: 10.1007/s12221-016-5838-8.
37. Kim, E.Y., Kim, D.S., & Ahn, B.T. (2009). Synthesis of mesoporous TiO₂ and its application to photocatalytic activation of methylene blue and E. coli. *Bull. Korean Chem. Soc.* 30(1), 193–196. DOI: 10.5012/bkcs.2009.30.1.193.
38. ALOthman, Z.A. (2012). A review: fundamental aspects of silicate mesoporous materials. *Materials* 5(12), 2874–2902. DOI: 10.3390/ma5122874.
39. Karimi, L. & Zohoori, S. (2013). Superior photocatalytic degradation of azo dyes in aqueous solutions using TiO₂/SrTiO₃ nanocomposite. *J. Nanostructure Chem.* 3(1), 1–5. DOI: 10.1186/2193-8865-3-32.
40. Mirjalili, M., Karimi, L. & Barari-tari, A. (2015). Investigating the effect of corona treatment on self-cleaning property of finished cotton fabric with nano titanium dioxide. *J. Text. Inst.* 106(6), 621–628. DOI: 10.1080/00405000.2014.932058.
41. Li, W., Wu, Z., Wang, J., Elzatahry, A.A. & Zhao, D. (2013). A perspective on mesoporous TiO₂ materials. *Chem. Mater.* 26(1), 287–298. DOI: 10.1021/cm4014859.